A reconfigurable complex band-pass filter with improved passive compensation*

Fan Chaojie(范超杰), Mo Tingting(莫亭亭)†, Chen Dongpo(陈东坡), and Zhou Jianjun(周健军)

Centre of Analog and Radio Frequency Integrated Circuits (CARFIC), Shanghai Jiao Tong University, Shanghai 200240, China

Abstract: This paper presents a 5th-order Chebyshev-I active RC complex filter for multi-mode multi-band global navigation satellite systems (GNSS) RF receivers. An improved passive compensation technique is used to cancel the excess phase lag of the integrators, thus ensuring the in-band flatness of the frequency response over various ambient conditions. The filter has a programmable gain from 0 to 42 dB with a 6 dB step, a tunable center frequency at either 6.4 MHz or 16 MHz, and a bandwidth from 2 to 20 MHz with less than 3% frequency uncertainty. Implemented in a 0.18 μm CMOS process, the whole filter consumes 7.8 mA from a 1.8 V supply voltage and occupies a die area of 0.4 mm^2.

Key words: complex filter; low-IF; multi-band GNSS; quality factor; passive Q compensation; frequency calibration

DOI: 10.1088/1674-4926/33/12/125004 **EEACC:** 1205; 1280

1. Introduction

Global navigation satellite systems (GNSS) have been widely used in navigation, positioning, surveying, synchronization, and many other applications. In GNSS RF receivers, low intermediate frequency (low-IF) architecture is preferred[1], which avoids problems like DC-offset, flicker noise, and LO-leakage in zero-IF receivers. However, the image interference problem becomes very challenging for low-IF receivers. To ensure good image rejection, high order complex filters are usually used to simultaneously implement channel selection, image rejection, and anti-aliasing[2]. In applications requiring high linearity performance, the active-RC filter is often a better circuit architecture rather than its G_m–C counterpart due to its feedback structure[2, 3]. However, there are two major non-idealities in active-RC filters: frequency deviation and Q enhancement. The former is caused primarily by process variations of on-chip capacitors and resistors, and also slightly by the limited OpAmp bandwidth, and can be precisely calibrated with low cost[5]. On the other hand, the Q enhancement effect is much more complex to analyze and eliminate, especially when poles with high quality factors exist in the filter's transfer function, such as in a high order, high centre frequency, narrow bandwidth complex filter.

The major reason for Q enhancement is the limited OpAmp gain-bandwidth (GBW) product, the higher the operating frequency and quality factor are, the more this factor is sensitive to the OpAmp's GBW, and the higher the ripple will be at this filter's cut-off frequency[6]. For a Chebyshev low-pass filter with $Q > 5$, the GBW of the OpAmp needs to be over 70 times higher than the cut-off frequency to suppress the pass-band ripple under 0.6 dB, not to mention complex filters with higher Qs than their low-pass prototypes. High bandwidth amplifiers consume very large power, which is far from acceptable in battery powered devices such as portable GPS receivers.

To meet the power budget, several Q compensation schemes[7–9] are developed to stabilize filters' quality factors, and thus their frequency responses. Active compensation schemes track the changes of ambient conditions, but require considerable extra power[7]. Traditional passive compensation is extremely simple, and power efficient, however, its effectiveness may deteriorate over different processes, temperatures, and supply voltages. Recently, adaptive passive compensations have been invented[8, 9], in which slave filters are usually employed to measure the Q deviation from its nominal value, and adaptively force it to zero by controlling some tunable circuits, then, according to good on-chip matching, the master filter is also well compensated by the same control word. These methods make use of a closed feedback loop, and add a moderate amount of extra power, but their circuit implementations are complicated, and often require mixed-signal techniques.

In this paper, we present a novel Q compensation scheme based on the traditional passive method. It directly makes use of the frequency calibration result, adapts to different processes and temperature conditions, but requires nearly no additional circuit complexity or power. A complex filter for GNSS receivers is fabricated and tested, to which this modified compensation is applied. With compensation, this filter achieves a sufficient in-band flatness of about 1 dB ripple height in different frequency configurations (for GPS, Galileo, and Compass), and low power to fit this portable application, simultaneously.

2. Non-ideal effects and practical issues

2.1. Frequency deviation

In active-RC filters, centre frequency and bandwidth are determined primarily by the values of resistors and capacitors, specifically, their product. On-chip resistors and capac-

* Project supported by the Chinese National Major Science and Technology Projects (No. 2009ZX01031-002-005).

† Corresponding author. Email: motingting@ic.sjtu.edu.cn

Received 5 April 2012, revised manuscript received 3 July 2012

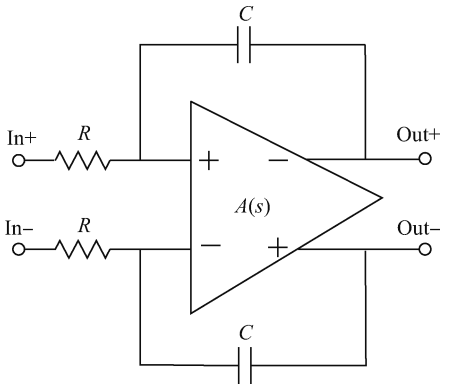

Fig. 1. Basic integrator circuit.

itors have about 15% error in their absolute values at process corners, in both directions, at extreme cases these errors can cause up to 40% frequency deviation, thus necessitating frequency calibration. Many frequency calibration schemes have been well developed and verified, and in this design we chose one of the most cost efficient approaches[5], as will be briefly described in Section 3.

Except for process variations, insufficient OpAmp bandwidth also lowers filter' frequency slightly, this effect is minor, and is usually neglected.

2.2. Q enhancement

The basic building element in active-RC filters is the integrator (Fig. 1), any non-ideal effect in filter leads to corresponding non-ideality in the integrator.

Taking the limited GBW into account, we can assume a first order model for the OpAmp's response $A(s)$ in the frequency range of interest (the range over which filter performance is of concern).

$$A(s) = \frac{A_0 p}{s + p}, \tag{1}$$

where A_0 is its DC gain, and p is the dominant pole, thus GBW $= A_0 p$. With this non-ideal OpAmp, the integrator transfer function becomes:

$$I(s) = \frac{-1}{\dfrac{s^2 RC}{\text{GBW}} + \left(\dfrac{RC}{A_0} + \dfrac{1}{\text{GBW}} + RC\right) s + \dfrac{1}{A_0}}. \tag{2}$$

This non-ideal integrator has a finite DC gain, slightly lower unit-gain frequency, and most important of all, different phase from the nominal 90 degree due to the second pole at high frequency. The effect of these non-idealities on a testing integrator's frequency response is shown by solid lines in Fig. 2, the simulation is based on an integrator with a unity gain frequency of 4 MHz, and an OpAmp of 500 MHz GBW, the ideal case is also plotted in dashed lines for comparison. In most cases, the magnitude response is very approximate to ideal before the frequency goes too high, while phase error comes much earlier; in high Q filters, in-band ripple at the vicinity of pass-band is very sensitive to this phase error, as will be explained.

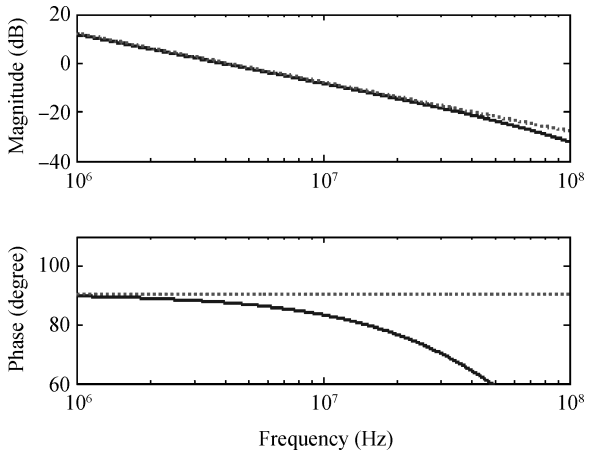

Fig. 2. Frequency response of ideal and non-ideal integrators (dashed line for the ideal case).

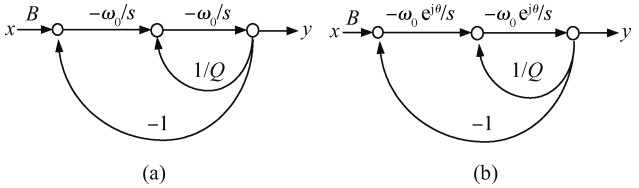

Fig. 3. Biquad SFG (a) ideal integrators and (b) integrators with phase error.

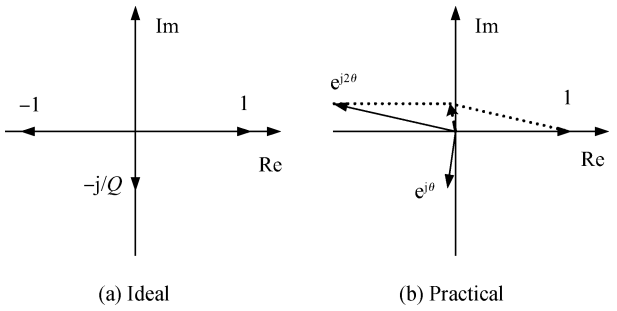

Fig. 4. Denominator vectors at ω_0.

To get an intuitive view of the Q enhancement effect, we focus on a simple second order filter (biquad), whose ideal transfer function and signal flow graph are expressed by Eq. (3) and Fig. 3(a).

$$B(s) = \frac{B_0 \dfrac{\omega_0^2}{s^2}}{1 + \dfrac{\omega_0}{Qs} + \dfrac{\omega_0^2}{s^2}}. \tag{3}$$

Figure 3(b) illustrates the same biquad, but with integrators having phase error. In the vicinity of its pass-band, say $s = \mathrm{j}\omega_0$, the denominator magnitude of Eq. (3) could be obtained by adding the three vectors: 1, ω_0/Qs and ω_0^2/s^2, as shown in Fig. 4.

In the ideal case, the magnitude response at ω_0 is exactly the quality factor Q. When the integrator has a phase error, the 1st and 3rd terms in the denominator of Eq. (3) do not cancel, instead, they tend to form a short vector that partly cancels

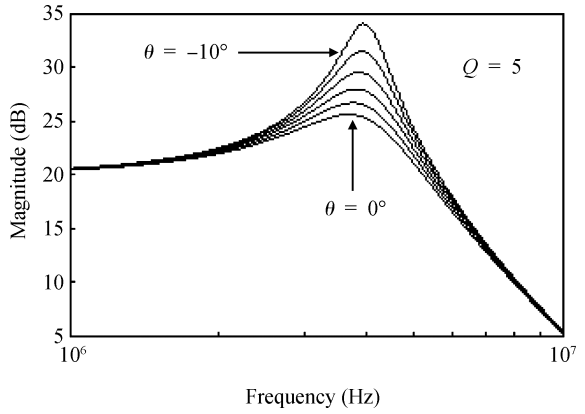

Fig. 5. Biquad response with different integrator phase lags.

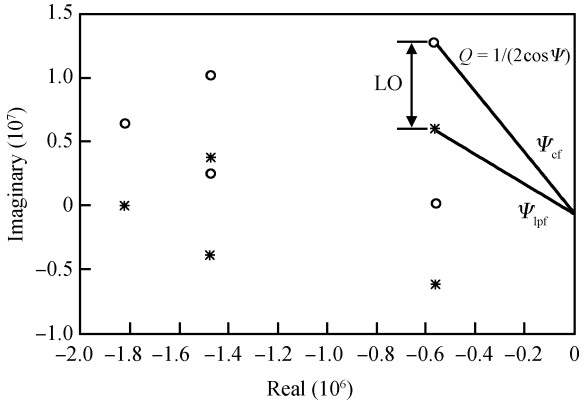

Fig. 6. Increase in Q when transferred to complex filter (LPF-star, CP-circle).

the 2nd term, in high Q biquads, this cancellation may greatly enhance magnitude response around ω_0, even leading to instability, this phenomenon is generally found in higher order filters, especially in complex band-pass filters whose quality factor is higher than their low-pass prototypes. Figure 5 shows the magnitude response of a biquad with $Q = 5$, assuming different amount of phase lags.

In the most stringent case of this design, the low-pass prototype filter with 2 MHz bandwidth has $Q = 5.56$, when shifted to a complex filter by LO = 6.4 MHz, Q will be increased to 11.2, so is its sensitivity to non-ideal effects. Figure 6 illustrates this situation.

3. Improved passive compensation

3.1. Frequency calibration

The simple frequency calibration scheme used in this design is not novel[5], but it directly assists the improved Q compensation discussed in the next sub-section. The basic concept of frequency calibration is to stabilize the on-chip RC time constants by tuning either capacitor or resistor arrays. The RC time constant in this design is found by measuring the time elapsed for a testing R-C network to be charged from 0 V to a certain voltage level, $V_{DD}/2$ in our case, as depicted in Fig. 7. A tunable capacitor array is continuously adjusted by a control word until this charging time approaches a set value (defined by a delay circuit); the other RC time constants on the same chip are calibrated by the same word due to on-chip matching. A 5-bit control word is used to cover the range from 75% to 140% of the nominal frequency, and allow the tuning accuracy to reach 2.5% of nominal.

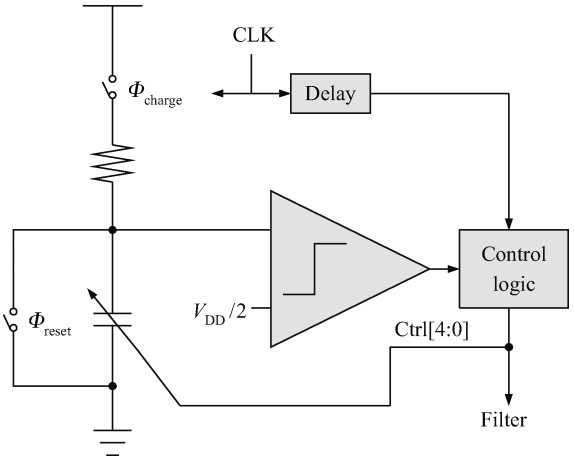

Fig. 7. Frequency calibration circuit.

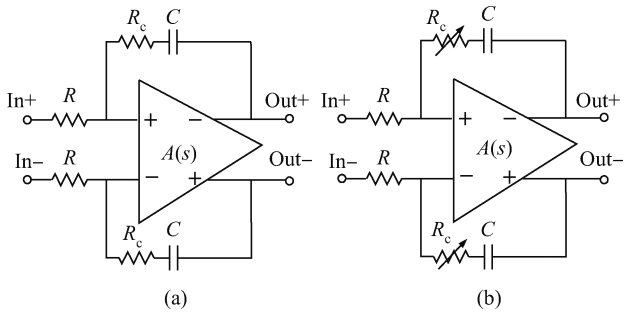

Fig. 8. Passive Q compensation. (a) Traditional. (b) Recently modified in Ref. [8].

3.2. Improved passive Q compensation

As was analyzed in Section 2.2, integrators' excess phase lag is the main reason responsible for Q enhancement, and this phase lag is introduced by its second pole at high frequency. To compensate this effect, a direct measure is to cancel this non-dominant pole. The traditional passive compensation inserts a series resistor with the feedback capacitor in integrators, thus introducing a zero to do this cancellation, as shown in Fig. 8(a), its transfer function is expressed by Eq. (4).

$$H(s) = \frac{-\dfrac{A_0 p}{RC}(1 + sCR_c)}{s^2 + s\left[\dfrac{1}{RC}(1 + sCR_c) + (A_0 + 1)p\right] + \dfrac{p}{RC}(1 + sCR_c)} \approx \frac{-\dfrac{A_0 p}{RC}(1 + sCR_c)}{s^2 + s\left[\dfrac{1}{RC}(1 + sCR_c) + (A_0 + 1)p\right]}. \quad (4)$$

The approximation is valid at high frequencies where the non-dominant pole resides. To reach complete cancellation, R_C

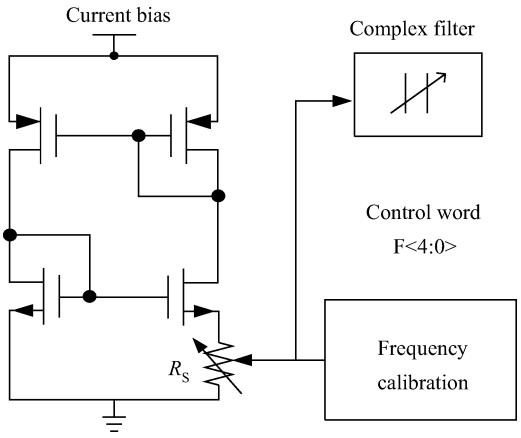

Fig. 9. Improvement of Q compensation.

should to be set at:

$$R_C = \frac{1}{C(A_0+1)p} \approx \frac{1}{C \times \mathrm{GBW}}. \tag{5}$$

However, since all of the resistors, capacitors, and OpAmp bandwidths are imprecise in value, this equality is fragile over process, temperature and supply voltage variations. To maintain the effectiveness of this passive compensation, an automatic adjustment scheme needs to be applied, in Ref. [8], the series resistor R_C is replaced by a tunable resistor array, see Fig. 8(b). A replica filter is used to measure the Q error and determine the control word applied to the array. However, in addition to a considerable amount of extra power and circuit complexity, this method may occupy a large die area. The reason for this is, for a good linearity performance, the R_C array must be a parallel one with the transistor switches located at the OpAmp's inputs. To ensure compensation accuracy, the least significant bit (LSB) parallel resistor needs to show very small conductance, that is a large resistance, since each differential integrator needs two such resistor arrays, and the entire complex filter will be unacceptably area consuming.

The improved Q compensation developed in this work makes use of the frequency calibration result in order to maintain the equality of Eq. (5). The concept is: during frequency calibration, the feedback capacitor array C is tuned to the point that the time constant CR is kept constant. Due to matching between R and R_C, CR_C is also fixed under different ambient conditions. According to Eq. (5), a tuning scheme is apparently needed to stabilize GBW, so that the passive compensation requirement is satisfied. As is widely known, the GBW of a Miller compensated OpAmp is determined by the ratio of input transistors' trans-conductance g_m, to the miller capacitor's value, if the OpAmp is biased by a constant-gm current source circuit, g_m will be inversely proportional to a certain resistor R_s in that circuit, so is the GBW. The principle of improved passive Q compensation can be described by the following equations:

$$R_{C_{\mathrm{nominal}}} = \frac{1}{C_{\mathrm{nominal}} \times \mathrm{GBW}_{\mathrm{nominal}}}, \tag{6}$$

$$\mathrm{GBW}_{\mathrm{nominal}} = \frac{g_{m_{\mathrm{nominal}}}}{C_{C_{\mathrm{nominal}}}} = \frac{\alpha}{R_{S_{\mathrm{nominal}}} \times C_{C_{\mathrm{nominal}}}}, \tag{7}$$

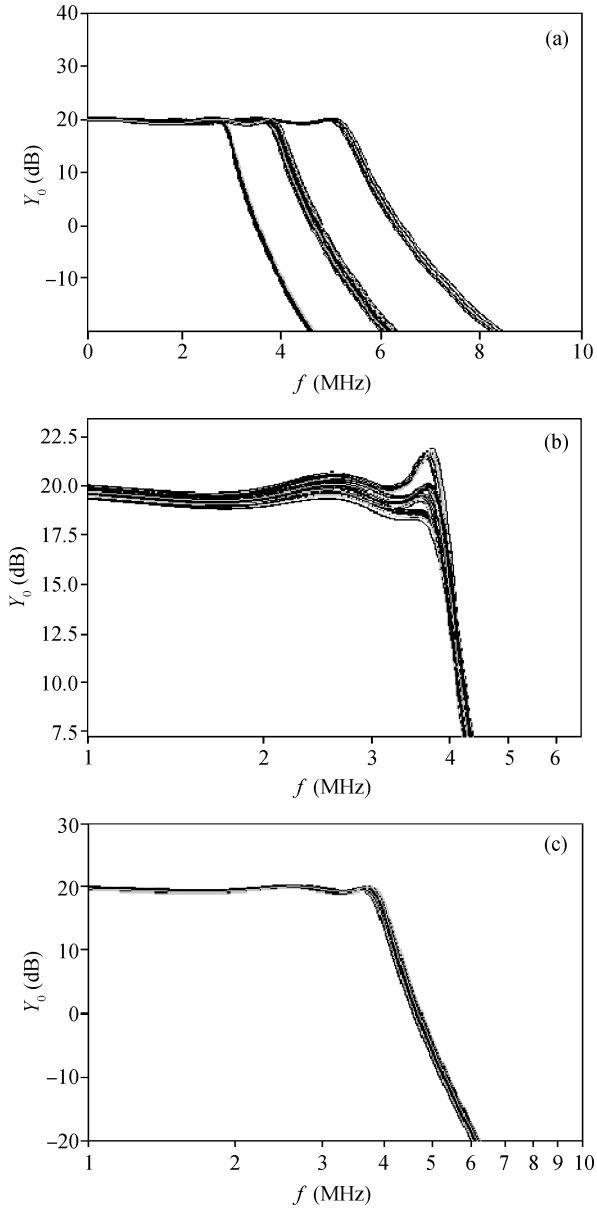

Fig. 10. Simulated magnitude response of a high Q testing filter (a) without calibration, (b) with only frequency calibration, or (c) with both calibration and Q compensation.

$$R_C = (1+e_r)R_{C_{\mathrm{nominal}}}, \tag{8}$$

$$R_S = (1+e_r)R_{S_{\mathrm{nominal}}}, \tag{9}$$

$$C = (1+e_r)C_{\mathrm{nominal}}, \tag{10}$$

$$C_C = (1+e_r)C_{C_{\mathrm{nominal}}}, \tag{11}$$

$$C_{\mathrm{tuned}} = \frac{C}{(1+e_r)(1+e_c)} = FC. \tag{12}$$

Here R_C, R_S, C, and C_C are imprecise practical values of the resistors and capacitors, α is a constant design parameter, F is the tuning factor obtained by frequency calibration. By

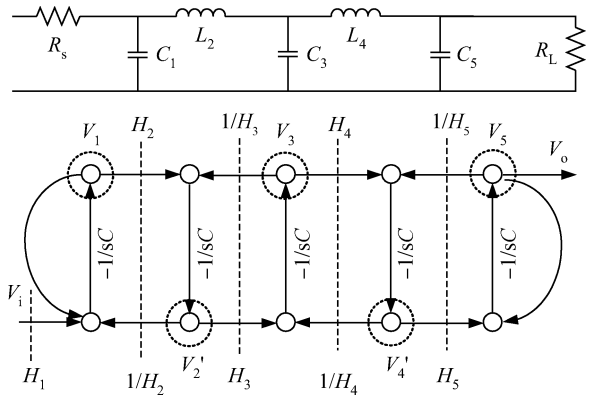

Fig. 11. Prototype LC filter and signal flow graph.

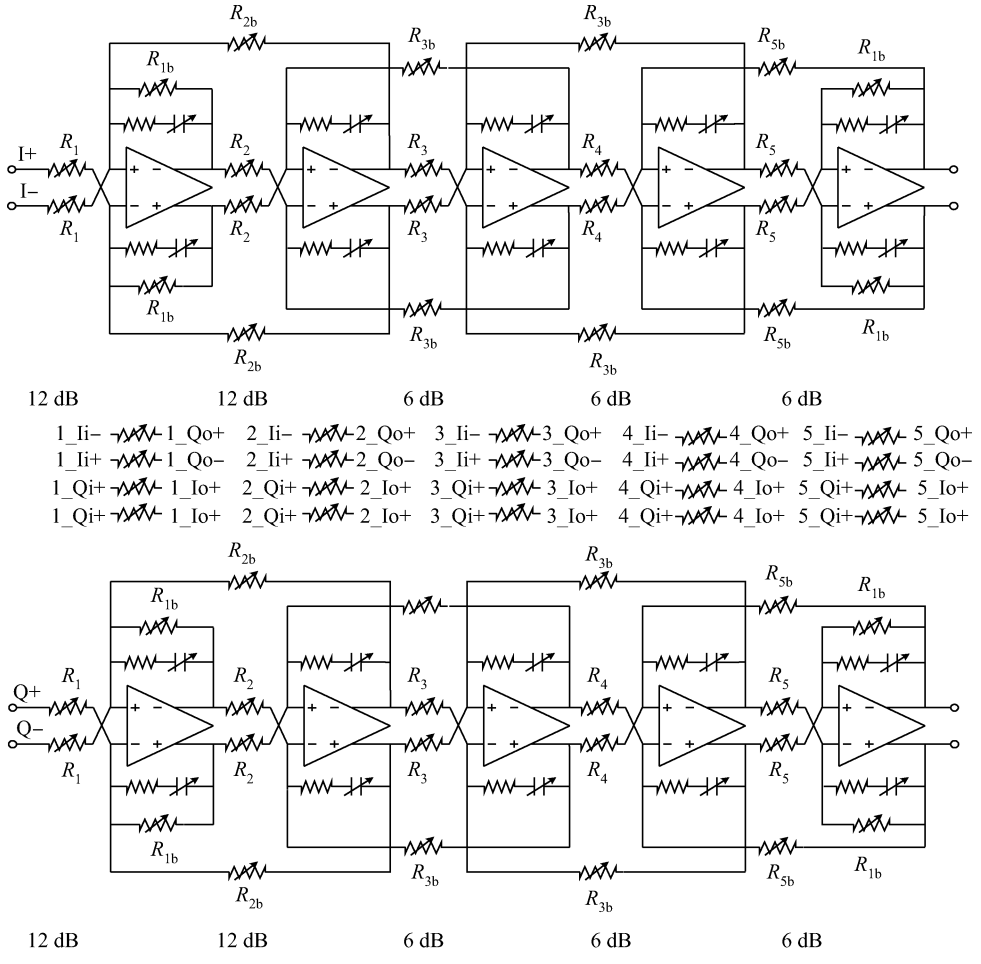

Fig. 12. Complex filter architecture (I/Q channels and cross R array).

simply applying this factor to R_S, the passive Q compensation can be maintained valid:

$$R_{S_{tuned}} = FR_S, \tag{13}$$

$$\mathrm{GBW}_{tuned} = \frac{\alpha}{C_C R_{S_{tuned}}} = \frac{1}{C_{tuned} R_C}. \tag{14}$$

Figure 9 conceptually describes this method.

Figures 10(a) to 10(c) compare the simulated magnitude responses of an LPF with $Q = 5.6$ without any calibration, with frequency calibration only, and with both frequency and improved passive Q compensation at different process corners, temperatures, and supply voltages, respectively.

It is obvious from the simulation that the improved passive Q compensation effectively stabilized the filter's quality factor and eliminated excess in-band ripple, while frequency calibration successfully limited frequency error to within ±2.5%.

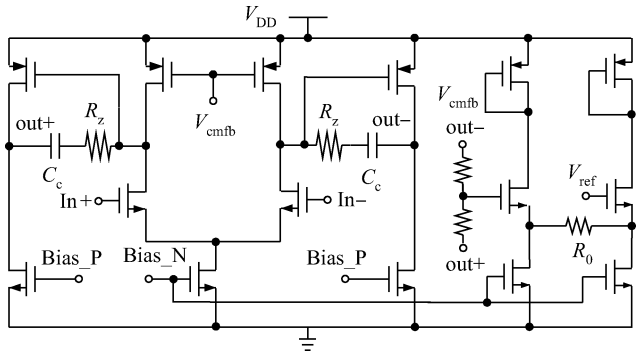

Fig. 13. Two-stage operational amplifier.

Up to now, the scheme seems to work without any cost. In fact, it does bring a potential problem to the OpAmp. When the current source is tuned, the GBW of the OpAmp stays at the wanted location. However, its non-dominant pole tends to move in a wider frequency range because the current changes, and this may deteriorate the stability of the feedback loop. To overcome this problem, a second constant-g_m circuit independent from the calibration word is added to provide current for the OpAmp's second stage, since the non-dominant pole is approximately determined by the ratio of the second stage's trans-conductance g_{m2} to the loading capacitor C, which is calibrated, it is roughly constant too. Complete simulation is performed over all PVT corners to make sure that phase and gain margins are adequate in any situation.

4. Circuit implementation

A 5th order Chebyshev I complex filter incorporating this compensation scheme is realized with integrated circuits. Figures 11 and 12 illustrate the design routine, from an LC prototype and signal flow graph (SFG), to the final complex filter architecture.

A total gain of 42 dB is properly distributed among the 5 stages during the trade off between noise and linearity performances. Most of the resistors are tunable arrays to facilitate programmable gain, bandwidth, and centre frequency.

A classical two-stage fully differential OpAmp with Miller compensation is adopted with a GBW of only 300 MHz, as shown in Fig. 13, notice that the first and second stages are separately biased so that Q compensation can be achieved without affecting the OpAmp's stability too much. Thus, the only cost of this compensation is a second constant-g_m current source, which only requires a tiny amount of additional power and die area, making it much more efficient than other compensation methods.

5. Experimental results

The proposed complex filter is fabricated in 0.18 μm CMOS technology, as a part of a GNSS wireless receiver. It occupies a die area of 1060 × 410 μm^2, and draws 7.8 mA from a 1.8 V supply. Figure 13 shows the filter's die photograph. The entire receiver has 28 dB image rejection, as can be seen in Fig. 14. The remaining image is due to inevitable component mismatches between I/Q channels. The programmability

Fig. 14. Photograph of the complex filter.

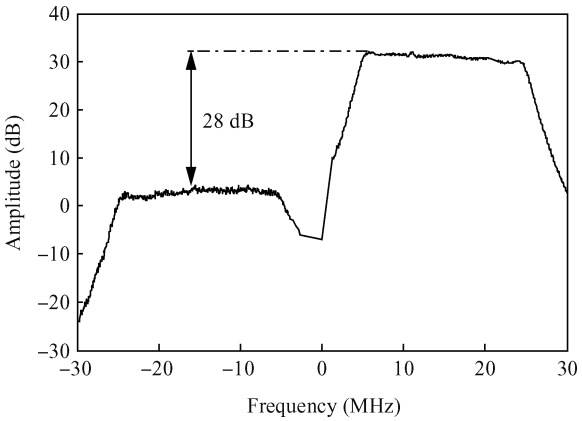

Fig. 15. Measured image rejection @ BW = 20 MHz, IF = 16 MHz.

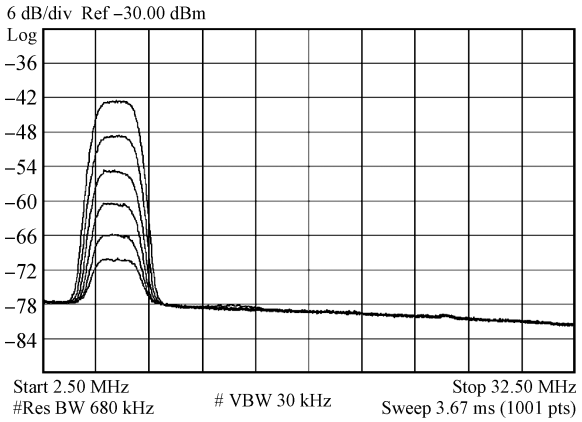

Fig. 16. Measured gain programmability @ BW = 2 MHz, IF = 6.4 MHz for GPS L1.

of this complex filter on gain, bandwidth, and center frequency are shown in Figs. 15–17. This complex filter can shift its centre frequency between 6.4 MHz and 16 MHz, and bandwidth among four different choices for each IF frequency. In each frequency mode, a gain range from 0 to 42 dB with 6 dB per step is covered. The in-band magnitude responses are quite flat in different configurations, taking into account the complex filter's high quality factor.

The key performances of the complex filter compared with other works are listed in Table 1.

Table 1. Performance summary.

Parameter	This work	Ref. [8]	Ref. [4]
Process	0.18 μm CMOS	0.13 μm CMOS	0.13 μm BiCMOS
Power supply (V)	1.8	1.5	2.5
Filter type	5th order Chebyshev	5th order Chebyshev	7th order Chebyshev
Area/channel (mm^2)	0.2	0.2	0.3
Power/channel (mA)	3.9	6	10.5
Centre frequency (MHz)	6.4/16	DC	DC
Bandwidth (MHz)	2–8/5–20	19.7	1.78–3.92
Gain range (dB)	0–42	N/A	0–40
Peak Q	11.2	4	6.2
In-band ripple (dB)	< 1	0.5	N/A

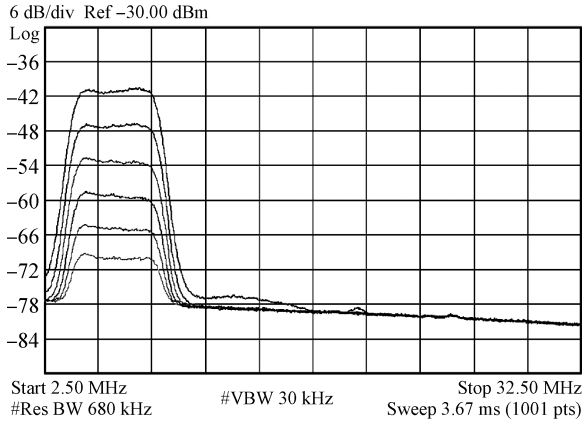

Fig. 17. Measured gain programmability @ BW = 4 MHz, IF = 6.4 MHz for Galileo E1 and Compass B1.

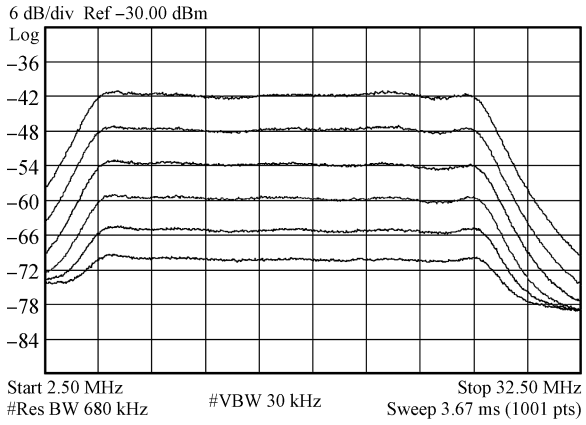

Fig. 18. Measured gain programmability @ BW = 20 MHz, IF = 16 MHz for GPS L5 and Galileo E5.

6. Conclusions

A 5th order Chebyshev-I complex filter for multi-mode GNSS RF receivers has been proposed and fabricated in 0.18 μm CMOS process. It has tunable BW (2, 4, 6, 8 MHz centers at 6.4 MHz or 5, 10, 15, 20 MHz centers at 16 MHz) and tunable gain (0 to 42 dB, 6 dB per step). The whole signal chain is able to receive signals in GPS L1/L2 bands (BW = 2, 20 MHz), Galileo E1/E5 bands (BW = 4, 20 MHz) and Compass B1 band (BW = 4 MHz). An improved passive compensation scheme is described and implemented to cancel the effects of various ambient environments on the Q compensation accuracy. According to theoretical analysis, the scheme will also be effective in other active RC filters.

References

[1] Wu J, Jiang P, Chen D, et al. A dual-band GNSS RF front-end with a pseudo-differential LNA. IEEE Trans Circuits Syst II, Express Briefs, 2011, 58(3): 134

[2] Wan C, Li Z, Hou N. A CMOS G_m–C complex filter with on-chip automatic tuning for wireless sensor network application. Journal of Semiconductors, 2011, 32(5): 055002

[3] Zou L, Liao Y, Tang Z. An eighth order channel selection filter for low-IF and zero-IF DVB tuner applications. Journal of Semiconductors, 2009, 30(11): 115002

[4] Yang Z, Wen G, Feng X. A 2.5-V 56-mW baseband chain in a multistandard TV tuner for mobile and multimedia applications. Journal of Semiconductors, 2011, 32(3): 035003

[5] Oshima T, Maio K, Hioe W, et al. Novel automatic tuning method of RC filters using a digital-DLL technique. IEEE J Solid-State Circuits, 2004, 39(11): 2052

[6] Khorramabadi H, Gray P. High-frequency CMOS continuous-time filters. IEEE J Solid-State Circuits, 1984, 19(6): 939

[7] Brackett P O, Sedra A S. Active compensation for high-frequency effects in opamp circuits with applications to active RC filters. IEEE Trans Circuits Syst, 1976, 23(2): 68

[8] Kousai S, Hamada M, Ito R, et al. A 19.7 MHz, fifth-order active-RC Chebyshev LPF for draft IEEE802.11n with automatic quality-factor tuning scheme. IEEE J Solid-State Circuits, 2007, 42(11): 2326

[9] Kallam P, Sinencio E, Karsilayan A. An enhanced adaptive Q-tuning scheme for a 100-MHz fully symmetric OTA-based band-pass filter. IEEE J Solid-State Circuits, 2003, 38(4): 585